

Potential Use of Distributed Acoustic Sensors to Monitor Fractures and Microseismicity at the FORGE EGS site

Robert J. Mellors, Christopher Sherman, Pengcheng Fu, John McLennan, Joseph Morris, Frederick Ryerson, and Christina Morency

Lawrence Livermore National Laboratory, 7000 East Avenue, Livermore, CA, 94550, USA

mellors1@llnl.gov

Keywords: EGS, FORGE, DAS, fiber optic, strain, fracture modeling, microseismic

ABSTRACT

Distributed fiber optic acoustic sensors (DAS) installed in boreholes have provided a new and data-rich perspective on fracturing processes and microseismicity created by stimulation. The use of fiber optic sensors is increasing in the oil and gas industry but less so at geothermal sites. These sensors measure strain (or strain rate) with high spatial resolution (~ 1 m) along the fiber and can survive extreme conditions. Here, we explore the information that these sensors may reveal in an Enhanced Geothermal System (EGS) system, which includes both low-frequency signals associated with fracture opening and high-frequency microseismic signals. As a test case, we use parameters from the FORGE site in Milford, Utah, which is expected to create a reservoir at a depth of roughly 2 km in a crystalline granite formation with temperatures of more than 175°C. The subsurface signals are simulated in two ways: 1) a massively parallel multi-physics code that is capable of modeling hydraulic stimulation of a reservoir with a pre-existing discrete fracture network, and 2) a parallelized seismic wave propagation code for high-frequency seismic signals created by microseismic activity. The objective is to understand how fracture geometry could be constrained with fiber optic sensors located both in the main borehole and in nearby monitoring boreholes, and how well microseismic events could be characterized in terms of locations and moment tensors.

1. INTRODUCTION

The Frontier Observatory for Research in Geothermal Energy (FORGE) site in Milford, Utah is a planned demonstration site of an enhanced geothermal system (EGS). The site will evaluate ways to extract energy from hot crystalline rocks that lack an active hydrothermal system. It will serve as a laboratory to test innovative ideas, sensors, and advanced modeling algorithms. One of the key challenges is to understand and quantify the geometry of the fracture system, which is necessary to guide the drilling of production wells to achieve sufficient circulation (Brown et al. 2012).

One promising sensor type is distributed acoustic sensors (DAS), which use fiber optics to measure strain (or strain rate) as a function of time along an optical fiber and is capable of measuring the high-frequency variations from seismic waves as well as lower-frequency strain. Fiber sensors are particularly useful in wells, as deployment is easier than deploying strings of geophones and the fiber has reduced interference with operations (Mateeva et al., 2014). This has led to increased adoption in the petroleum industry. In the petroleum industry, DAS fiber data are used to monitor stimulations and borehole flow, record vertical seismic profiles (VSP), and measure microseismic events (Karrenbach et al, 2018). A more recent development is the ability to measure low-frequency strain ϵ (< 0.05 Hz) associated with the opening and closing of fractures (Jin and Roy, 2017; Hull et al., 2017). DAS sensors are often deployed with distributed temperature sensors (DTS) or distributed strain sensors (DSS), which rely on a different scattering mechanism and have different resolution.

The basic principle behind DAS relies on Rayleigh scattering. An interrogator box sends laser pulses down the fiber, where imperfections in the fiber backscatter small portions of each pulse as they pass through the fiber. These reflections return to the interrogator box where the phase is measured. Variations in the returned phase over time provide measurements of the strain at all points along the fiber (Hartog, 2017). The sensitivity and resolution, both spatial and temporal, are sufficient to capture a wide range of signals, from near DC to transient strains from seismic waves, in ideal conditions. We note that these distributed sensors are fundamentally different from fiber Bragg sensors, which are also fiber-based but are point sensors.

As the sensor records axial strain along the fiber, DAS data differs significantly from a standard seismic sensor. The strain (or strain rate) is measured as an average over segments, defined as the gauge length. The gauge length is controlled by the parameters of the laser pulses and implementation but typically ranges between 1 and 15 m. The spacing between measurements, generally referred to as the channel distance, can be shorter than the gauge length. For straight fibers, the response is at a maximum for seismic waves travelling parallel to the fiber but decreases sharply at angle and roughly as $\cos^2\theta$ where θ is the angle with respect to the fiber axis. It is possible to deploy the fiber in a helix to reduce the azimuthal dependency. Another problem occurs when wavelengths are near, or less than the gauge length, in which case spatial aliasing will corrupt the signal (Dean et al., 2017). Current DAS sensors have higher instrumental noise floors than seismic sensors but appear to have a wider frequency response than geophones.

Fiber sensors also have potential for robust performance at high temperatures, which is essential for geothermal applications. As all of the electronics are on the surface, it only the fiber and surrounding cable need to be resistant. Silica glass is extremely resistant to high temperature (up to 800°C), but typical polymer coatings are not and it is necessary to use polyamide coatings at elevated temperatures ($\sim 250^\circ\text{C}$). Metal coated fibers (e.g. aluminium, copper, or gold) are possible but have issues with performance. As a result, little use of

DAS has been made in geothermal wells, although a related technology, distributed temperature sensing, has been deployed (e.g. Patterson et al., 2017, Petty et al., 2013) and provided useful constraints on injection flow. Reinsch et al., (2016) deployed a fiber optic cable in a well in the Reykjanes geothermal field, Iceland and also recorded surface data from unused telecom fiber. Fiber DAS data were also collected at the Brady geothermal field (Miller et al., 2018). Most of the DAS data were collected on the surface although 400 m of fiber was deployed inside a well.

This combination of ease of deployment and resistance to high temperatures makes fiber sensors a promising choice for EGS monitoring. In this work we use numerical models to explore what might be possible to measure with DAS sensors at an EGS site. We focus on fracture imaging. Two possible approaches exist: 1) direct measurement of the strain field created by fractures as they open (and close); and 2) measurements of the microseismic events triggered by the stimulation and how well they can be located and characterized. DAS sensors located in the injection borehole itself can be used to infer areas of flow or as a basis for VSP surveys, but we will not cover these topics in this paper. Installation is also a separate topic and here we assume that fibers are cemented in place. This should be straightforward for monitoring wells or cased injection wells; fiber deployment in uncased wells is possible but with significant impacts on sensitivity.

Our synthetic examples are inspired by the setting of the FORGE project but are intended only to illustrate potential fiber measurements using highly simplified models. The images here should not be taken to represent expected FORGE results due to the simplifications in the models presented here. Currently, an initial FORGE well (58-32) has been drilled. It is vertical and extends to a depth of 2,297 m. The upper section of the well lies in granite alluvium. At a depth of 975 m, the well enters the Miocene diorite, granodiorite, and granite of the Mineral Mountain batholith after a short transition through 50 m of weathered granite. Suitable reservoir conditions (based on temperatures of 175° C) were encountered at a depth of 1980 m in crystalline granite (Balamir et al., 2018; FORGE Report, 2018). In the initial phases of the project, two vertical monitoring wells will be drilled to depths of roughly 305 and 914 m and referred as the shallow and intermediate monitoring wells. These will be offset to the east of well 58-52, approximately 300-400 m away. The intermediate well will penetrate the top of the granite and extend roughly 30 m into the granite. At later stages, additional monitoring wells may be drilled. In this paper we show how modeling can inform future well positions.

2. METHOD

As mentioned above we evaluate two methods of estimating fracture extent based on DAS measurements: low-frequency strain and microseismic data. Low-frequency strain from hydraulic fractures in unconventional hydrocarbon stimulations has been observed (e.g. Jin and Roy, 2017; Karrenbach et al., 2018) although care must be taken to remove other possible low-frequency strain signals induced in the fiber by effects such as temperature variations. This would require co-located distributed temperature sensing, for example. The fiber would also likely need to be cemented in. If conditions permit observation, this would allow direct imaging of the fracture extent and estimation of aperture. Figure 1 shows a simplified example illustrating how a rectangular fracture propagating horizontally would appear on two vertical monitoring wells. In this work we will explore what might be expected in a scenario similar to FORGE.

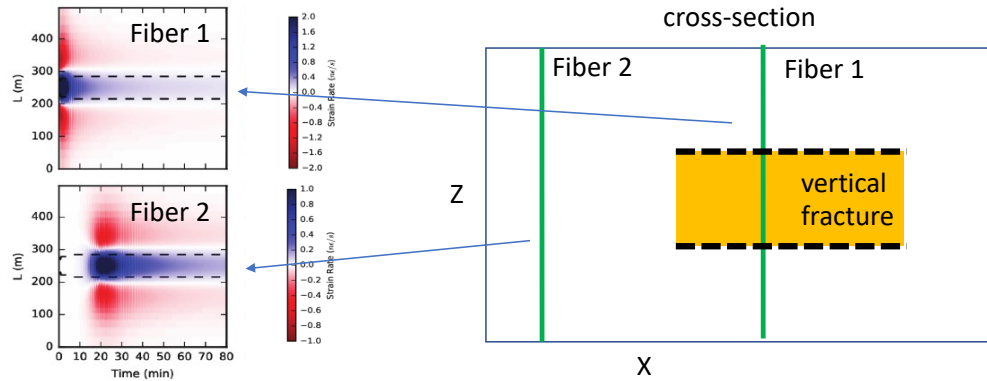


Figure 1: Example schematic view of expected low-frequency signal as observed at two fibers near a vertical rectangular fracture propagating horizontally between two barriers (change in stress or material properties). The plots on the left show the strain signal as a function of depth and time. The transition between blue and red matches the fracture extent and the amplitude is proportional to change in the fracture aperture. The delay between the injection start and the initial strain recorded at fiber 2 represents the fracture propagation velocity towards the fiber.

The second method is mapping of the microseismic events associated with the fracture opening. While DAS offers significant advantages in deployment and spatial resolution over geophones, it also includes disadvantages. The noise floor is typically higher than for geophones (at least for the current generation of interrogators) and the single component of measured strain restricts interpretation. The sensitivity of the fiber decreases as the incidence angle increases, with very little sensitivity to broadside signals. The gauge length of the fiber also impacts response when the apparent wavelength approaches the gauge length. Despite these effects, microseismic events can often be clearly imaged using DAS and the high spatial resolution leads to dramatic images of the wavefield. Unfortunately, a single straight DAS fiber cannot uniquely define a hypocenter (Karrenbach et al., 2018). Here we generate example synthetics and show that if the hypocenter is known it is possible invert for a moment tensor.

2.1 Fracture models

We conduct some basic fracture models using GEOS, a multi-physics software package designed to simulate 3D reservoir stimulation. It employs a fully coupled finite element/finite volume approach to model initiation, propagation, and reactivation of fractures, both existing fractures and hydraulically-driven, new fractures, within arbitrarily complex 3D fracture geometries (Settgast et al., 2017, Fu et al., 2014). GEOS has been validated with numerous analytic solutions and extensively applied to hydraulic stimulation models for oil and gas and EGS geothermal models. Here we build some simple models representative of the FORGE geology but using an arbitrary injection scheme.

In the baseline simulation, we assume the rock has a Young's modulus $E=50$ GPa and Poisson's ratio $\nu=0.2$. The average fracture gradient, namely the vertical gradient of the minimum horizontal principal stress S_{hmin} , is 14 kPa/m. In the baseline simulation, we superpose a random perturbation onto the S_{hmin} profile. The perturbation has spatially autocorrelated variations with a zero mean and is generated following the method described in Guo et al. (2016). The standard deviation is 1.0 MPa, with correlation lengths of 200 m and 100 m in the horizontal and vertical directions, respectively. The rock is assumed to have a critical stress intensity factor, commonly known as the toughness of the rock, $KIC=2$ MPa \cdot m^{0.5}. We assume that the injection point is at an elevation of -630 m. The stimulation consists of an injection of fluid with a dynamic viscosity of 100 cP at 53 L/s (20 BPM) for 300 minutes. As the fracture gradient is 40% greater than the hydrostatic gradient of water, the in situ stress profile tends to drive upward height growth in the absence of counter-mechanisms.

To model expected low-frequency DAS signal, we insert a virtual fiber-optic sensor on which we will measure synthetic low-frequency DAS signals, following the approach given in Sherman et al. (2019). This should match the strain observed on a fiber inserted in a monitoring well with that geometry. The strain along the fiber is estimated and then convolved with a rectangular function to match the effect of the gauge length. The advantage of the virtual fiber is that various geometries can be tested to evaluate sensitivity. This virtual fiber is vertically oriented, spans the full-depth of the model, and is offset 0 m and 50 m in the x- and y-directions, respectively, from the point of fluid injection. After 300 minutes of stimulation, the fracture has propagated outward and mostly upward. The aperture varies, as it is controlled by the random perturbations in S_{hmin} . Figure 2 shows a series of snapshots that show the growth of the hydraulic fracture in the x-z plane and the position of the virtual fiber-optic sensor, which is located 50 m away in the y direction. Figure 3 shows the synthetic low-frequency DAS measurements along the virtual fiber associated with the fracture shown in Figure 2. The change in the strain field associated with growth of the fiber is clearly visible in the fiber data and changes in amplitude represent variations in fracture aperture. The upper edge of the fracture generates a clear signal as it expands upward. The lower edge only generates a signal in the initial growth period. Taken together, the strain measurements can be interpreted to estimate the fracture geometry over time and constrain aperture.

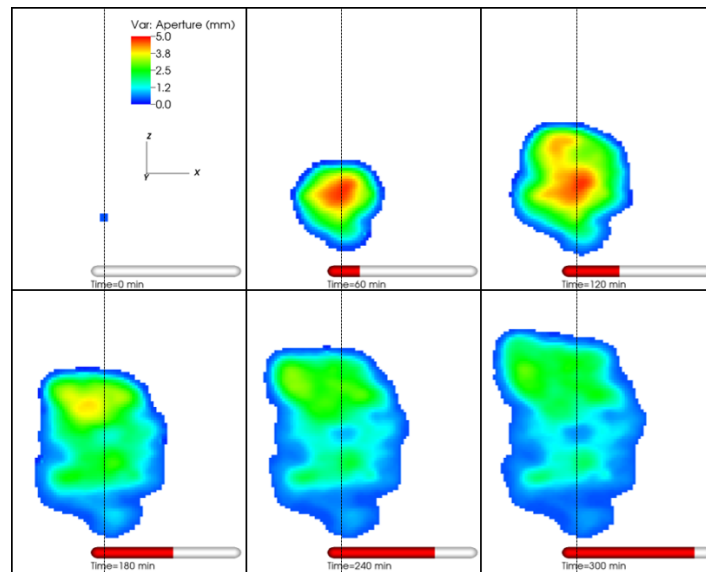


Figure 2: Snapshots showing the growth of the hydraulic fracture, with the colormap showing the fracture aperture, which varies as a result of the imposed heterogeneous stress field. The virtual monitoring well is located 50 m away (in y direction) from the injection point, which has created a fracture in the x-z plane and is expanding mostly upward. The injection is assumed to last for 300 minutes.

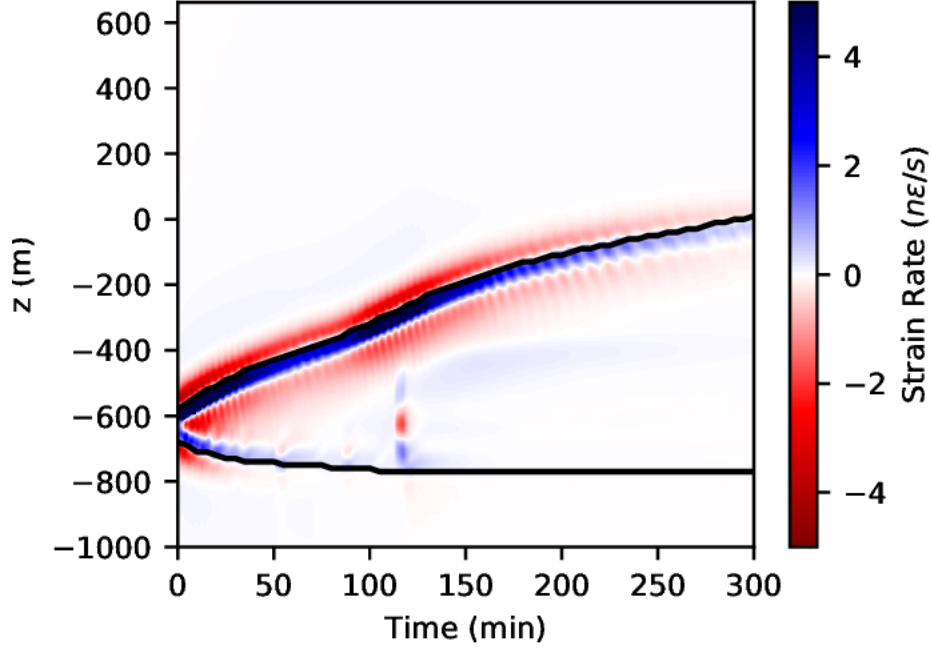


Figure 3: Synthetic low-frequency DAS measured for the target fiber (50 m away) in the hydraulic fracturing model. The solid black lines indicate the vertical extents of the hydraulic fracture over time. Note that the upper part of the fracture, which is growing upward over time, displays a stronger signal than the lower edge, which remains relatively static.

2.2 Microseismic

Here we present the synthetic microseismic events as measured on a vertical fiber. We assume a homogenous medium and a vertical fiber (Figure 4). A microseismic event is located 200 m from the fiber in the y direction and 100 m above the deepest fiber channel (Figure 4). Waveforms (vertical strain as a function of time) are calculated using SPECfEM, an open source spectral-element wave propagator code (Komatitsch and Tromp, 1999). The strain tensor is calculated based on the spatial derivation of the displacement and waveforms calculated for 101 channels assuming a spacing of 6 m (Figure 5). We use the forward waveforms calculated for a given moment tensor as data recorded on the vertical fiber, and tested a full waveform linear inversion to recover the moment tensor using a known location (Kikuchi and Kanamori, 1991).

Figure 5 shows an example waveform as recorded on the vertical fiber. Note the P and S waves which appear as two cones with the apex at the depth of the event. The distance can be calculated using a velocity model and the S-P difference. Unfortunately, with this data alone it is not possible to calculate a unique location as any location at that depth and distance (effectively, a circle) could fit the data (Karrenbach et al., 2018).

If we assume that the location is known (perhaps by using other data), it is possible to invert the waveforms for a moment tensor. First, we generate a series of synthetics for a set of selected moment tensors and then add noise to the data to test sensitivity. The noise is generated using a Gaussian function convolved with a series of randomly distributed numbers in the range [0,1] and then scaled to 10% and 20% of the maximum amplitude of the strain signal across the set of moment tensors tested, and added to the strain time series.

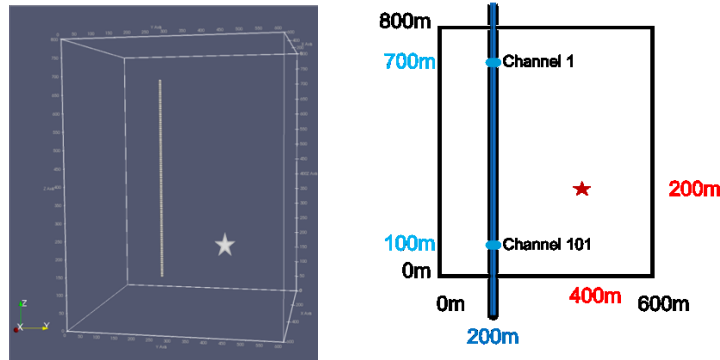


Figure 4: Geometry of the synthetic vertical fiber and microseismic event location. The model is 600m, 600m and 800m in x, y and z-directions, respectively.

Table 1 shows the results of the inversion on noisy data. Focal mechanism solutions as well as the 6 moment tensor components are displayed, with the decomposition into double coupled (dc), compensated linear vector dipole (clvd) and isotropic (iso) components. Results show that the focal mechanisms are still resolved but the presence of noise in the data affects the resolution in the isotropic, dc, and clvd components. The fit also decreases drastically due to the presence of noise in the data. We are evaluating how the use of helical fiber or a curved fiber might allow for improved moment tensor inversion without requiring other data.

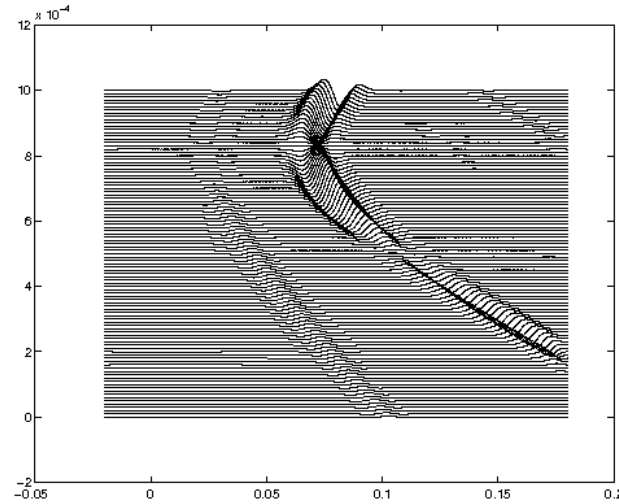


Figure 5: Example of vertical strain recorded at channels 0 to 101 with no noise added.













	Case 1	Case 2	Case 3	Case 4
0%				
S/N	-	-	-	-
Fit	0.974611	0.999296	1.000000	0.999999
%iso, dc, clvd	0, 99, 1	0, 99, 1	100, 0, 0	0, 100, 0
10%				
S/N	0.08	10.00	1.29	9.72
Fit	0.000343	0.402905	0.074780	0.425507
%iso, dc, clvd	6, 88, 6	7, 84, 9	92, 2, 6	7, 89, 4
20%				
S/N	0.04	5.00	0.64	4.86
Fit	0.000281	0.246250	0.022929	0.272298
%iso, dc, clvd	12, 77, 11	13, 71, 16	88, 2, 10	13, 78, 9

Table 1: Results of moment tensor inversion with fixed location using data with 0%, 10% and 20 % noise. The signal-to-noise, fit, and the % decomposition into isotropic, double-couple, and compensated linear dipole are displayed.

3. RESULTS

We conclude that monitoring with fiber in monitoring wells near the depth of the expected fractures could potentially resolve low-frequency strain thereby allowing constraints on the fracture geometry. Microseismic monitoring will be useful but should be supplemented with geophones due to limitations in hypocenter accuracy using only vertical fiber data. This difficulty might be alleviated by a curved deployment of fiber or possibly a helically wound fiber.

For the upcoming shallower monitoring wells, a substantial change in rock properties occurs at the alluvium/crystalline interface with an increase in seismic wave velocity from 3.8 km/s to 5.5 km/s (compressional) and a corresponding increase in S wave velocities. We expect that seismic signals will be attenuated by the impedance contrast. A short section of the intermediate well will extend into the granite but

as fiber optic relies on averaged signals over a gauge length, likely less than 5 gauge lengths will be within the granite which will make robust interpretation difficult. It would be useful to extend deeper into the granite to yield a longer length of fiber.

Acknowledgements. This work was performed under the auspices of the U.S. Department of Energy by Lawrence Livermore National Laboratory under Contract DE-AC52-07NA27344 and was supported by the LLNL-LDRD Program under Project No. 17-ERD-015 (R.M., C.S., C. M., J.M, F.R). Funding for this work was provided by the U.S. DOE EERE GTO under grant DE-EE0007080 “Enhanced Geothermal System Concept Testing and Development at the Milford City, Utah FORGE Site”. We thank the many stakeholders who are supporting this project, including Smithfield, Utah School and Institutional Trust Lands Administration, and Beaver County as well as the Utah Governor’s Office of Energy Development (J.L). Contribution LLNL-CONF-767223.

REFERENCES

- Balamir, O., Rivas, E. Rickard, W.M., McLennan, J., Mann, M., and Moor, J.: Utah FORGE Reservoir: Drilling Results of Deep Characterization and Monitoring Well 58-32. (2018), Proceedings of the 43rd Workshop on Geothermal Reservoir Engineering, Stanford University, Stanford, California, February 12-14, 2018. SGP-TR-213
- Brown D. W., Duchane, D. V, Heiken G, Hrisu V.T. : Mining the earth’s heat: hot dry rock geothermal energy. (2012) Springer, New York. <https://doi.org/10.1007/978-3-540-68910-2>
- Dean, T., Cuny, T., and Hartog, A. H.: The effect of gauge length on axially incident P-waves measured using fibre optic distributed vibration sensing, *Geophysical Prospecting*, 65, (2017), 184–193. doi:10.1111/1365-2478.12419
- Frontier Observatory for Research in Geothermal Energy Milford Site, Utah, Phase 2B Final Topical Report. (2018), EGI at the University of Utah.
- Fu, P., Settgast, R. R., Johnson, S. M., Walsh, W. D. C., Morris, J. P., and Ryerson, F. J.: GEOS: User Tutorials, LLNL-TR-665515, (2014), 94 pages.
- Guo, B., Fu, P., Hao, Y., Peters, C.A., and Carrigan, C. R : Thermal Drawdown-Induced Flow Channeling in a Single Fracture in EGS., (2016), *Geothermics* 61: 46–62.
- Hartog, A. H.: An Introduction to Distributed Optical Fibre Sensors, CRC Press, (2017), 442 pages.
- Hull, R. A., Meek, R., Bello, H., and Miller, D.: Case History of DAS Fiber-Based Microseismic and Strain Data, Monitoring Horizontal Hydraulic Stimulations Using Various Tools to Highlight Physical Deformation Processes (Part A), URTeC: 2695282, DOI 10.15530/urtec-2017- 2695282.
- Jin, G. and Roy, B.: Hydraulic-fracture geometry characterization using low-frequency DAS signal. *Leading Edge*, 36(12), 975–980. <https://doi.org/10.1190/tle36120975.1>
- Karrenbach, M., Ridge, A., Cole, S., Boone, K., Kahn, D., Rich, J. Silver, K., Langton, D.: Fiber-optic distributed acoustic sensing of microseismicity, strain and temperature during hydraulic fracturing, (2018), *Geophysics*, 84, D11-D23. doi:10.1190/geo2017-0396.1
- Kikuchi, M. and Kanamori, H.: Inversion of complex body waves-III, (1991), *Bull. Seismol. Soc. Am.*, 81, 2335–2350.
- Komatitsch, D. and Tromp, J.: Introduction to the spectral-element method for 3-D seismic wave propagation, (1999), *Geophys. J. Int.*, 139, 806–822.
- Mateeva, A., Lopez, J., Potters, H., Mestayer, J., Cox, B., Kiyashchenko, D., Wills, P., Grandi, S., Hornman, K., Kuvshinov, B., Berlang, W., Yang Z., and Detomo, R.: Distributed acoustic sensing for reservoir monitoring with vertical seismic profiling, *Geophysical Prospecting*, (2014), 62, 679–692
- Miller, D., Coleman, T. and the POROTOMO team, DAS and DTS at Brady Hot Springs: Observations About Coupling and Coupled Interpretations, (2018), PROCEEDINGS, 44th Workshop on Geothermal Reservoir Engineering. Stanford University, Stanford, California, February 12-14, SGP-TR-213.
- Patterson, J. R., Cardiff, M., Coleman, T., Wang, H., Feigl, K. L., Akerley, J., Spielma, P.: Geothermal reservoir characterization using distributed temperature sensing at Brady Geothermal Field, Nevada, *Leading Edge* 36, 12(2017), 1024a1-1024a7 <https://doi.org/10.1190/tle36121024a1.1>
- Petty, S., Nordin, Y., Glassley, W., Cladouhos, T. T., and Swyer, M., Improving geothermal project economics with multi-zone stimulation: results from the Newberry Volcano EGS demonstration, Proceedings, Thirty-eighth Workshop on Geothermal Reservoir Engineering, Stanford University, Stanford, California, Feb. 11-13, 2013, SGP-TR-198
- Reinsch, T., Jousset, P., Henninges, J. Blanck, H.: Distributed Acoustic Sensing Technology in a Magmatic Geothermal Field - First Results From a Survey in Iceland, *Geophysical Research Abstracts*, (2016), 18, EGU2016-16670, EGU General Assembly 2016
- Settgast, R. R., Fu, P., Walsh, S. D. C., White, J. A., Annavaraou, C., and Ryerson, F. J.: A fully coupled method for massively parallel simulation of hydraulically driven fractures in 3-dimensions, *Int. J. Numer. Anal. Meth. Geomech.*, 41, (2017), 627–653. doi: 10.1002/nag.2557.
- Sherman, C., Mellors, R., Morris, J., and Ryerson, R.: Geomechanical Modeling of Distributed Fiber-Optic Sensor Measurements. Interpretation, 7, (2019), 1-7. doi: 10.1190/INT-2018-0063.1